



Title	Tuning of the Optoelectronic Properties for Transparent Oxide Semiconductor ASnO(3) by Modulating the Size of A-Ions
Author(s)	Wei, Mian; Cho, Hai Jun; Ohta, Hiromichi
Citation	ACS Applied Electronic Materials, 2(12), 3971-3976 https://doi.org/10.1021/acsaelm.0c00806
Issue Date	2020-12-22
Doc URL	https://hdl.handle.net/2115/83637
Rights	This document is the Accepted Manuscript version of a Published Work that appeared in final form in ACS Applied Electronic Materials, copyright © American Chemical Society after peer review and technical editing by the publisher. To access the final edited and published work see https://pubs.acs.org/doi/10.1021/acsaelm.0c00806 .
Type	journal article
File Information	Revised Supporting Information_201125.pdf, Supporting Information



Supporting information

Tuning of the optoelectronic properties for transparent oxide semiconductor ASnO_3 by modulating the size of A-ions

Mian Wei^{1*}, Hai Jun Cho^{1,2}, and Hiromichi Ohta^{1,2*}

¹*Graduate School of Information Science and Technology, Hokkaido University, N14W9, Kita, Sapporo 060–0814, Japan*

²*Research Institute for Electronic Science, Hokkaido University, N20W10, Kita, Sapporo 001–0020, Japan*

Mian Wei

ORCID: orcid.org/0000-0001-9793-4325

Email: wm3256@gmail.com

Hiromichi Ohta

ORCID: orcid.org/0000-0001-7013-0343

Email: hiromichi.ohta@es.hokudai.ac.jp

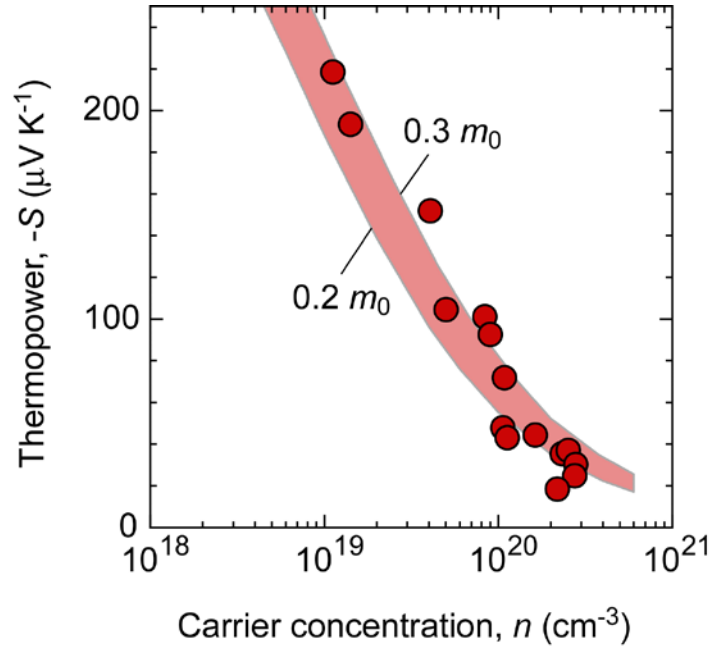


Figure S1. Thermopower ($-S$) of the resultant films as a function of carrier concentration (n) at room temperature. The carrier effective mass (m^*) of the films are in the range from 0.2 to 0.3 m_0 .

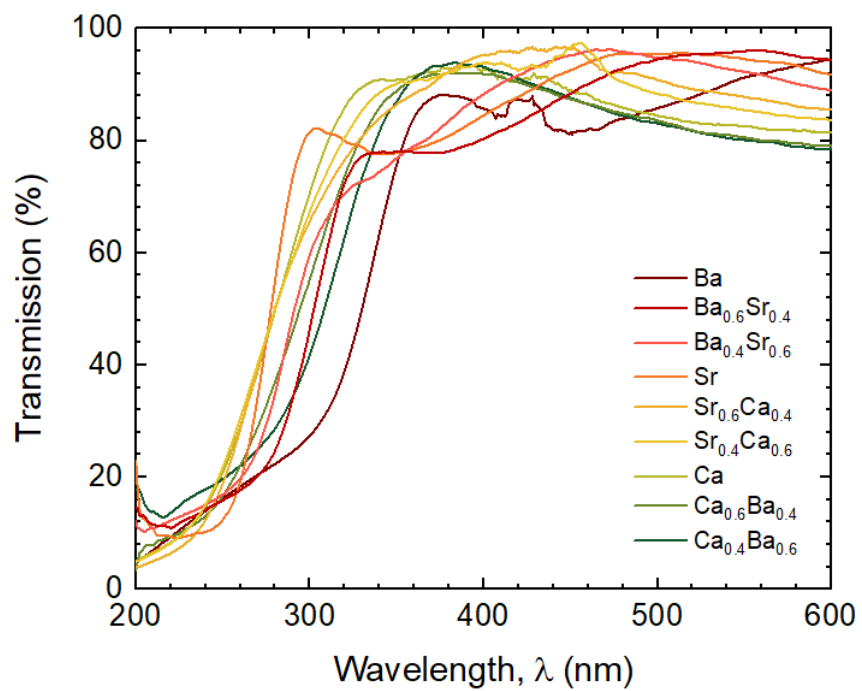


Figure S2. Optical transmission spectra of the resultant films (film thickness: 100nm).

Table S1. Crystallographic analyses of the resultant films.

Composition	Average ionic radius of A-site ion (Å)	$(a^2c)^{1/3}$ (Å)	D (nm)
CaSnO ₃	1.34	3.949	20.2
Ca _{0.8} Sr _{0.2} SnO ₃	1.36	3.973	21.1
Ca _{0.6} Sr _{0.4} SnO ₃	1.38	4.002	23.5
Ca _{0.4} Sr _{0.6} SnO ₃	1.40	4.014	17.6
Ca _{0.2} Sr _{0.8} SnO ₃	1.42	4.031	31.1
SrSnO ₃	1.44	4.033	33.6
Sr _{0.8} Ba _{0.2} SnO ₃	1.47	4.052	22.4
Sr _{0.6} Ba _{0.4} SnO ₃	1.51	4.092	24.2
Sr _{0.4} Ba _{0.6} SnO ₃	1.54	4.132	27.7
Sr _{0.2} Ba _{0.8} SnO ₃	1.58	4.107	31.3
BaSnO ₃	1.61	4.138	24.3
Ba _{0.8} Ca _{0.2} SnO ₃	1.56	4.129	24.6
Ba _{0.6} Ca _{0.4} SnO ₃	1.50	4.090	27.0
Ba _{0.4} Ca _{0.6} SnO ₃	1.45	4.066	39.1
Ba _{0.2} Ca _{0.8} SnO ₃	1.39	3.998	22.7

D : lateral coherence length

Table S2. Optical transmission in wavelength of 260 nm and bandgap of the resultant films.

Composition	Transmission, T (%)	E_g (eV)
CaSnO ₃	28.9	4.64
Ca _{0.8} Sr _{0.2} SnO ₃	29.2	4.66
Ca _{0.6} Sr _{0.4} SnO ₃	30.4	4.66
Ca _{0.4} Sr _{0.6} SnO ₃	28.1	4.57
Ca _{0.2} Sr _{0.8} SnO ₃	26.8	4.53
SrSnO ₃	15.1	4.43
Sr _{0.8} Ba _{0.2} SnO ₃	13.6	4.25
Sr _{0.6} Ba _{0.4} SnO ₃	18.0	4.17
Sr _{0.4} Ba _{0.6} SnO ₃	17.0	3.97
Sr _{0.2} Ba _{0.8} SnO ₃	16.6	3.77
BaSnO ₃	18.3	3.59
Ba _{0.8} Ca _{0.2} SnO ₃	23.3	3.73
Ba _{0.6} Ca _{0.4} SnO ₃	22.2	3.99
Ba _{0.4} Ca _{0.6} SnO ₃	21.8	4.35
Ba _{0.2} Ca _{0.8} SnO ₃	28.5	4.55

Table S3. Activation energy of the electrical conductivity for the resultant films.

Composition	E_a (meV)
$\text{Ca}_{0.7}\text{Sr}_{0.3}\text{SnO}_3$	22.25
$\text{Ca}_{0.5}\text{Sr}_{0.5}\text{SnO}_3$	3.12
$\text{Ca}_{0.4}\text{Sr}_{0.6}\text{SnO}_3$	-1.49
$\text{Ca}_{0.3}\text{Sr}_{0.7}\text{SnO}_3$	-5.55
$\text{Ca}_{0.2}\text{Sr}_{0.8}\text{SnO}_3$	-5.78
$\text{Ca}_{0.1}\text{Sr}_{0.9}\text{SnO}_3$	-7.58
SrSnO_3	-20.11
$\text{Sr}_{0.8}\text{Ba}_{0.2}\text{SnO}_3$	-2.17
$\text{Sr}_{0.6}\text{Ba}_{0.4}\text{SnO}_3$	-2.65
$\text{Sr}_{0.4}\text{Ba}_{0.6}\text{SnO}_3$	-10.14
$\text{Sr}_{0.2}\text{Ba}_{0.8}\text{SnO}_3$	-11.14
BaSnO_3	-14.48
$\text{Ba}_{0.8}\text{Ca}_{0.2}\text{SnO}_3$	-5.61
$\text{Ba}_{0.6}\text{Ca}_{0.4}\text{SnO}_3$	-0.12
$\text{Ba}_{0.4}\text{Ca}_{0.6}\text{SnO}_3$	13.68